# POLITECNICO DI TORINO
# Repository ISTITUZIONALE

A Monte Carlo multimodal inversion of surface waves

(Article begins on next page)

05 August 2020

# A Monte Carlo multimodal inversion of surface waves

## Margherita Maraschini and Sebastiano Foti

*Politecnico di Torino–DISTR, Corso Duca Degli Abruzzi* 24, 10129 *Torino, Italy. E-mail: margherita.maraschini@polito.it*

## SUMMARY

The analysis of surface wave propagation is often used to estimate the *S*-wave velocity profile at a site. In this paper, we propose a stochastic approach for the inversion of surface waves, which allows apparent dispersion curves to be inverted. The inversion method is based on the integrated use of two-misfit functions. A misfit function based on the determinant of the Haskell–Thomson matrix and a classical Euclidean distance between the dispersion curves. The former allows all the modes of the dispersion curve to be taken into account with a very limited computational cost because it avoids the explicit calculation of the dispersion curve for each tentative model. It is used in a Monte Carlo inversion with a large population of profiles. In a subsequent step, the selection of representative models is obtained by applying a Fisher test based on the Euclidean distance between the experimental and the synthetic dispersion curves to the best models of the Monte Carlo inversion. This procedure allows the set of the selected models to be identified on the basis of the data quality. It also mitigates the influence of local minima that can affect the Monte Carlo results. The effectiveness of the procedure is shown for synthetic and real experimental data sets, where the advantages of the two-stage procedure are highlighted. In particular, the determinant misfit allows the computation of large populations in stochastic algorithms with a limited computational cost.

**Key words:** Inverse theory; Probability distributions; Elasticity and anelasticity; Surface waves and free oscillations; Site effects; Wave propagation.

GJI Seismology

## 1 INTRODUCTION

The knowledge of the shear wave velocity ($V_s$) profile is valuable information for geotechnical characterization, geo-hazard studies, vibration propagation modelling and seismic site response studies (Kramer 1996). It can also be used to design filters for ground roll removal and for static calculation in seismic reflection processing (Mari *et al.* 1984).

Dispersivity of surface waves is widely used to infer the $V_s$ profile of a soil deposit. The velocity of high-frequency components depends on the mechanical parameters of the shallow portion of the subsoil, whereas low-frequency components travel with a velocity that also depends on the properties of deeper layers.

Surface wave propagation is a multimodal phenomenon. For a given subsoil model, each frequency can travel with several velocity values. The curves in the frequency–velocity space representing the propagation modes of the model are called modal dispersion curves and they depend only on model parameters. Often the fundamental mode (the slowest one) is the most energetic. In some cases, also higher modes are relevant and they can be used in the inversion process.

A variety of testing setup can be used to collect surface wave data, and dispersion curves can be extracted from the records using signal-processing tools (e.g. Dziewonski & Hales 1972; Nolet & Panza 1976; McMechan & Yedlin 1981).

Notwithstanding the relevance of higher modes, in surface wave analysis retrieving the $V_s$ profile from the fundamental mode of the observed dispersion curve is still quite common. Although this approach works fine in several cases, it does not allow all available information to be exploited. When a sharp velocity contrast or a velocity inversion are present, fundamental mode inversion can also generate sound errors due to mode misidentification (Maraschini *et al.* 2010). The apparent dispersion curve is given by the superposition of modal curves because of limitations in the array resolution (Gucunski & Woods 1992; Tokimatsu 1997; Foti *et al.* 2000).

Several authors have highlighted the importance of higher modes in the inversion process. They can be used to increase penetration depth (Gabriels *et al.* 1987; Xia *et al.* 2003; Ernst 2008), to stabilize the inversion process (Xu *et al.* 2006) and to enhance the resolution in $V_s$ of the inverted model (Xia *et al.* 2006). They are more sensitive than the fundamental mode on some model parameters (Socco & Strobbia 2004).

Other authors have focused on practical problems arising from the inclusion of higher modes in the inversion process. The first problem to deal with is the mode separation during processing. Gabriels *et al.* (1987) and Foti *et al.* (2000) highlighted the importance of a large number of sensors and a long array to improve spectral resolution while also retaining high-frequency information. When a two-station method is used (or a limited number of receivers), only an apparent dispersion curve can be retrieved (Tokimatsu *et al.* 1992;

Tokimatsu 1997). The mode separation can further be improved by means of signal-processing techniques. Park *et al.* (1999) and Luo *et al.* (2008) proposed, respectively, a wavefield transformation and a high-resolution linear Radon transform.

The major problem in multimodal dispersion curve inversion is mode numbering. A branch of the apparent dispersion curve can derive from the superposition of modes, or some modes may be misidentified in the experimental data set. Zhang & Chan (2003) remarked on the consequences of mode misidentification. If part of the dispersion curve is associated with an incorrect mode number, in particular in the low-frequency range, the consequent errors are greater than errors due to inaccuracy. From these considerations, we can derive the necessity for a multimodal inversion algorithm that does not require mode numbering.

To solve this problem, some authors (e.g. Ganji *et al.* 1998; Lai & Rix 1999; Forbriger 2003a,b) compared the experimental apparent dispersion curve with a synthetic apparent dispersion curve or used the full waveform inversion. These approaches are computationally expensive because they require a more realistic simulation of the wave propagation.

An approach for the inversion of multiple modes without the need to number modes was proposed by Ernst (2007) and successively implemented within a deterministic algorithm by Maraschini *et al.* (2010). This approach uses a misfit function based on the properties of the solution of the forward problem, allowing for a substantial saving of computational costs. In this paper, we implement the same misfit function within a stochastic algorithm.

The solution of an inverse problem is a probability density function on the model space, which can present several local minima (Socco & Boiero 2008). To find the model associated with the maximum probability, deterministic or stochastic algorithms can be used. The choice depends on the nature of the problem, the number of unknowns and the available computational resources (Sambridge & Mosegaard 2002). The main advantage of Monte Carlo inversion is that the assumption of linearity between data and model is not required (Sambridge & Mosegaard 2002; Socco & Boiero 2008). For non-linear inverse problems, such as surface wave analysis, the uniqueness of the solution is not guaranteed (Menke 1989) and a deterministic algorithm can converge into a local minimum because the model parameter space is not entirely explored (Curtis & Lomax 2001). Consequently, deterministic algorithms are suitable when *a priori* information can be used to constrain the solution. When the probability density function presents several local minima, and no *a priori* information is available, Monte Carlo methods are more suitable because they allow the whole model space to be investigated. Nevertheless deterministic inversion algorithms are computationally efficient, whereas Monte Carlo algorithms are computationally intensive because of the huge number of models that should to be tested to provide a meaningful result. For this reason, Monte Carlo algorithms require efficient forward models.

Several global search algorithms can be used, for example uniform sampling, Markov chain Monte Carlo, simulated annealing, genetic algorithms and neighbourhood algorithm (Sen & Stoffa 1996; Sambridge 1999a,b; Sambridge & Mosegaard 2002).

In the case of surface wave analysis, the forward operator of the dispersion curve calculation is a non-linear function. Consequently, a Monte Carlo algorithm is more suitable than a deterministic one, in particular when higher modes are considered, because the multimodal misfit function presents several local minima.

Song & Gu (2007) proposed a genetic algorithm for the characterization of a roadbed structure. A multimodal approach was required for the inversion because of a low-velocity layer in the subsoil

model, which would have led a fundamental mode inversion to an unrealistic result. The used misfit function was a weighted root mean squares distance between the observed and the calculated dispersion curves for each mode. This approach required mode numbering for the inversion.

Lu & Zhang (2006) proposed a multimodal algorithm able to avoid the problem of mode jumps for the inversion of dispersion curves generated by soil profiles presenting low-velocity layers. They compared the observed dispersion curve with a theoretical dispersion curve calculated choosing for each frequency the mode associated with the maximum displacement. A genetic algorithm, which avoids the dependences on the initial model, was used for the inversion. This method is slower but more accurate than root mean squared multimodal inversion because modal misidentification is avoided.

Ryden & Park (2006) studied surface waves on pavements, and they remarked on the importance of multimodal analysis and the problem of mode numbering. They proposed a fast simulated annealing algorithm, which compares the observed and the modeled phase-velocity spectra. This approach required the displacements calculation, which is computationally expensive.

In this paper, a multimodal misfit function that avoids modal misidentification and does not require displacements calculation is presented. The proposed misfit function does not require the modal dispersion curve calculation because it is based on the function whose zeroes are dispersion curve for the calculation of the misfit; consequently the forward code is very fast.

This misfit function is implemented within a uniform sampling algorithm, which is less efficient than other methods, but it mitigates the risk of falling into local minima. A second criterion to select a set of equivalent profiles accounting for data uncertainty is applied on the results of Monte Carlo inversion.

## 2 METHOD

### 2.1 The probabilistic approach to the inversion

The forward problem is the prediction of the motion parameters when a complete physical description of the model is given. The inversion problem is the inference of the model parameters given the results of measurements. If the forward operator is not an injective function from the model space to the data space, the inverse problem is not a function from the data space to the model space, because certain data can be generated by more than one model.

The general solution of an inverse problem is a probability distribution on the model space. This probability distribution is a combination of the experimental data, the *a priori* information about parameters and the theoretical model (Tarantola & Valette 1982; Mosegaard & Tarantola 1995; Tarantola 2005).

Let us call M the vectorial space containing all the possible models $\mathbf{m} = [m_1, \ldots, m_{Nm}]^{\mathrm{T}}$, where $N_m$ is the dimension of the space M and D the vectorial space containing all the possible data

$$\mathbf{D} = \begin{bmatrix} d_{1,1} & \cdots & d_{1,Nd} \\ \cdots & \cdots & \cdots \\ d_{N,1} & \cdots & d_{N,Nd} \end{bmatrix},$$

where $N_d$ is the number of parameters of a given data point and $N$ is the number of the data points.

The *a posteriori* probability $\sigma(\mathbf{m})$ of a model $\mathbf{m}$ can be calculated as (Mosegaard & Tarantola 1995):

$$\sigma(\mathbf{m}) = k_1 \rho(\mathbf{m}) L(\mathbf{m}), \tag{1}$$

where $\rho(\mathbf{m})$ is the *a priori* probability on the model space, $k_1$ is a normalization constant and $L(\mathbf{m})$ is the likelihood function, that is a function that describes the goodness of fit between the observed data and the theoretical data. As suggested by Mosegaard & Tarantola (1995), the likelihood function can be calculated from a misfit function $S(\mathbf{m})$, which represents a distance between the observed data and the synthetic data calculated from the model, as

$$L(\mathbf{m}) = k_2 \exp(-S(\mathbf{m})), \qquad (2)$$

where $k_2$ is a normalization constant.

## 2.2 The probabilistic approach applied to surface wave inversion

For surface wave inversion, the model is typically a stack of homogeneous linear elastic layers. The vector $\mathbf{m}$ contains model parameters of the layers (thickness, $V_s$, $V_p$ or Poisson ratio, and density). In the inversion, densities and Poisson ratio values are typically fixed to realistic *a priori* values, whereas layer thicknesses and $V_s$ values are the unknowns.

The matrix of the observed data contains the velocity–frequency couples of the observed dispersion curve, that is

$$\mathbf{D}^{obs} = \begin{bmatrix} v_1^{obs} & f_1^{obs} \\ \cdots & \cdots \\ v_N^{obs} & f_N^{obs} \end{bmatrix}. \qquad (3)$$
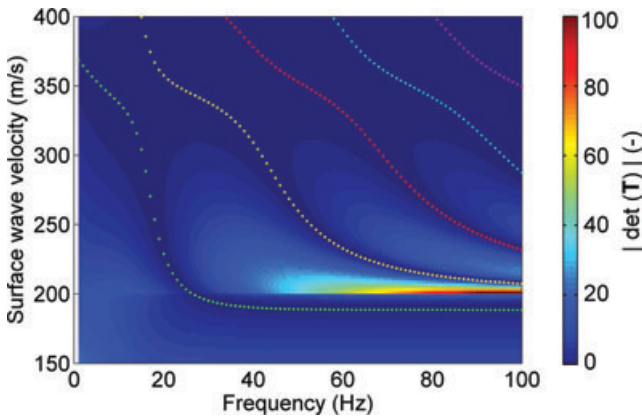


**Figure 1.** Absolute value of the Haskell–Thomson matrix determinant for a single layer (thickness: 5 m, density: 1800 kg m$^{-3}$, $V_s$: 200 m s$^{-1}$, $V_p$: 500 m s$^{-1}$) over a half-space (density: 1800 kg m$^{-3}$, $V_s$: 400 m s$^{-1}$, $V_p$: 800 m s$^{-1}$).

In this work, the chosen *a priori* probability for the model space $\rho(\mathbf{m})$ is a uniform distribution of the parameters in a given range: each parameter $m_i$ can vary between the given boundaries $m_i^{top}$ and $m_i^{bot}$, that is the *a priori* probability is a uniform probability on a hyperrectangle of dimension $N_m$ (Curtis & Lomax 2001). Range for the model parameters are selected on the basis of experimental data.

The function $S(\mathbf{m})$ is calculated using a forward operator. For the forward problem solution of Rayleigh and Scholte waves the Haskell–Thomson transfer matrix method is adopted (Thomson 1950; Haskell 1953; Haskell 1964), with the modifications proposed by Dunkin (1965); Gilbert & Bachus (1966); Herrmann & Wang (1980) and Herrmann (2002). The same methodology can be applied to other surface and interface waves, such as Love waves, and to other propagator matrix methods, like the stiffness matrix method (Kausel & Roesset 1981) and the Reflection-Transmission method (Kennet 1974; Kennet & Kerry 1979).

A transfer matrix is evaluated for each layer of a given model $\mathbf{m}^*$. The product of these matrices, together with the matrices of boundary conditions, is the Haskell–Thomson matrix $\mathbf{T}$ (Buchen & Ben-Hador 1996). The determinant of this matrix is a function of frequency and velocity, from the space MxD to real numbers:

$$F = |\det(\mathbf{T}(v, f, \mathbf{m}))|. \qquad (4)$$

For a given model $\mathbf{m}^*$, the function $|\det(\mathbf{T}(v, f, \mathbf{m}^*))|$ is a surface in the velocity–frequency domain. This function presents several local minima, corresponding to the modal dispersion curves of the model $\mathbf{m}^*$ (Fig. 1). For a given frequency $f^*$, $|\det(\mathbf{T}(v, f^*, \mathbf{m}^*))|$ is a continuous function which is zero if and only if $v$ belongs to a mode of the dispersion curve of the model $\mathbf{m}^*$ at the frequency $f^*$.

## 2.3 The determinant misfit function

For a given model $\mathbf{m}^*$ and a given observed data $\mathbf{D}_{obs}$, the misfit $S(\mathbf{m}^*)$ can be defined as the norm (in the following the norm L$^1$ is considered) of the values of the determinant of the $\mathbf{T}$ matrix evaluated in correspondence of the points of the observed dispersion curve (Ernst 2007; Maraschini *et al.* 2010) (see Fig. 2).

This misfit function presents two important advantages. First of all, this approach is inherently multimodal: it allows all the modes of the experimental dispersion curve to be considered, without the need to establish *a priori* to which mode each data point belongs to.

The second advantage is the computational cost, which is strongly reduced with respect to inversion algorithms adopting the usual misfit function based on the distance between the observed and the
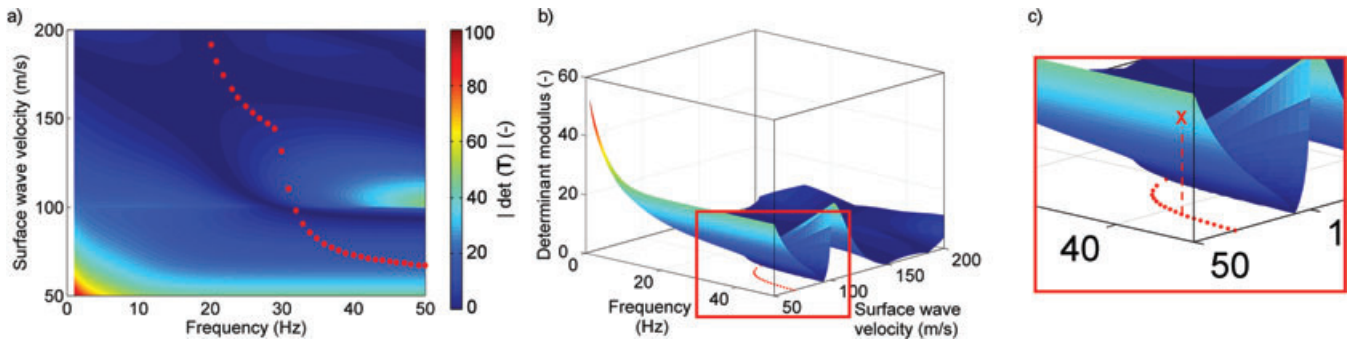


**Figure 2.** Representation of the determinant misfit function—(a) experimental dispersion curve (red dots) compared to the determinant misfit surface of a synthetic model $\mathbf{m}^*$; (b) 3-D view of (a); (c) zoom of (b): the red dots are the experimental dispersion curve, and the surface represents the absolute value of the determinant of a synthetic model $\mathbf{m}^*$; the point indicated with X is the absolute value of the determinant of the synthetic model $\mathbf{m}^*$ in correspondence of an experimental point; this value is the misfit of $\mathbf{m}^*$ for the single experimental point.

numerical dispersion curves of the model $\mathbf{m}^*$. Dispersion curve calculation requires a cost expensive zero search: for each frequency of the observed dispersion curve a zero search on velocity (or wavenumber) is required. The algorithm needs to be very accurate, because modes can be very close to each other, in particular in presence of sound stiffness contrasts, but it should also be efficient, because the forward problem is solved several times in the inversion, in particular when stochastic algorithms are applied. The zero search procedure requires several evaluations of the Haskell–Thomson matrix (the number depends on the complexity of the soil model and on the required accuracy) for each frequency. On the contrary, the proposed approach requires, for the evaluation of the misfit $S(\mathbf{m}^*)$, a single evaluation of the Haskell–Thomson matrix determinant for each frequency, and consequently the computational cost is reduced.

### 2.4 Estimate of uncertainty due to non-uniqueness

The solution of a deterministic inversion process is the model with the lowest misfit. One of the advantages of stochastic inversions is that the ensemble of profiles showing low misfit can provide a significant insight into the uncertainty associated with solution non-uniqueness. Nevertheless, the selection of a representative number of best-fitting profiles is not straightforward.
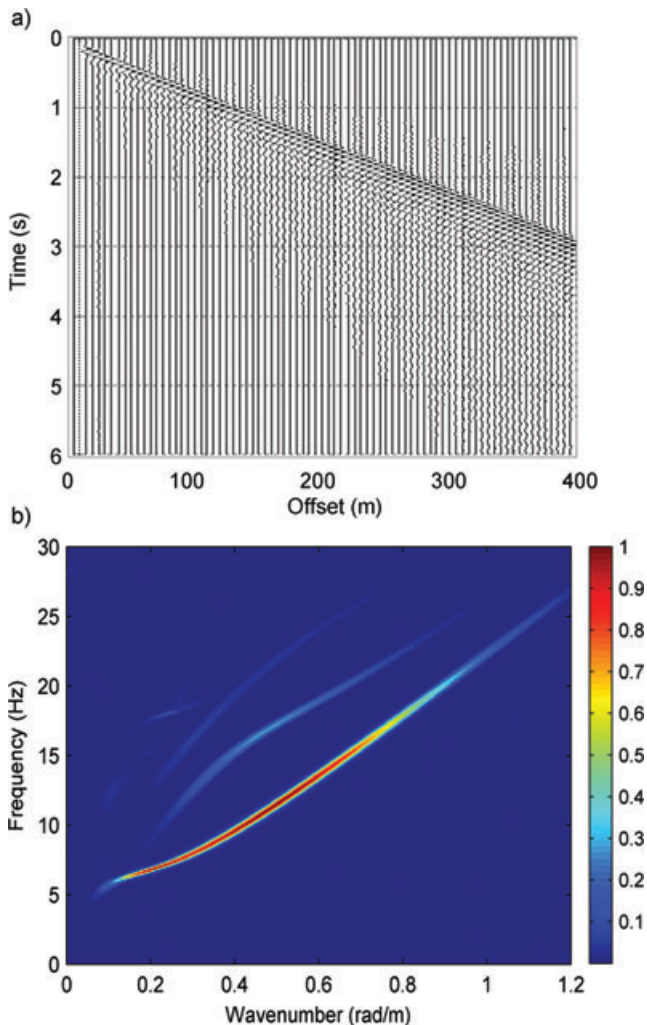


**Figure 3.** Case 1: (a) synthetic seismogram; (b) f–k spectrum.

**Table 1.** Characteristics of the synthetic models.

| Layer | Density (kg m$^{-3}$) | Poisson ratio (–) | *S*-wave velocity (m s$^{-1}$) | Thickness (m) |
|---|---|---|---|---|
| Model 1 | | | | |
| 1 | 1800 | 0.33 | 150 | 10 |
| 2 | 2100 | 0.27 | 450 | 390 |
| Model 2 | | | | |
| 1 | 1800 | 0.33 | 150 | 10 |
| 2 | 2000 | 0.27 | 280 | 20 |
| 3 | 2100 | 0.27 | 450 | 770 |

A second misfit function based on the distance between the experimental and the synthetic dispersion curves is used for the selection of acceptable profiles. This misfit function allows a statistical test to be applied.

It can be assumed that the experimental dispersion curve is affected by a Gaussian error (Lai *et al.* 2005) with known standard deviation (Socco & Boiero 2008). Under this assumption, we can define the misfit as:

$$\hat{S}(\mathbf{m}) = \frac{\sum_{i=0}^{N} [v_{\exp}(f_i) - v_{teor}(f_i)]^2 W(f_i)(\sigma_{\exp}(f_i))^{-2}}{N - (2n - 1)}, \quad (5)$$

where $v_{\exp}(f_i)$ and $v_{\text{teor}}(f_i)$ are, respectively, the experimental dispersion curve evaluated at the *i*th frequency and the closer mode of the theoretical dispersion curve evaluated at the same frequency; $W(f_i)$ and $\sigma_{\exp}(f_i)$ are, respectively, the weight and the uncertainty associated with the *i*th point of the experimental dispersion curve. Eq. (5) represents a misfit function based on the Euclidean distance between the experimental and the synthetic dispersion curves. It has the structure of a chi-square with $N$ and $2n – 1$ degrees of freedom, where $N$ is the number of data points in the dispersion curve and $n$ is the number of layers of the model (including the half-space). As there are no reasons to assume that the determinant has a Gaussian error, the determinant value could not be used instead of the distance between curves to build a chi-square distribution.

The acceptance criterion is based on the Fisher test (Socco & Boiero 2008). A generic model $\mathbf{m}$ is accepted if

$$F_\alpha(N - (2n - 1), N - (2n - 1)) < \frac{\hat{S}(\mathbf{m}_{best\,MC})}{\hat{S}(\mathbf{m})}, \quad (6)$$

where $F$ is the Fisher distribution, and $\alpha$ is the level of confidence of the test, which depends on data uncertainties.

For the application of the Fisher test to the Monte Carlo results, the following strategy is adopted. First, the profiles are ordered for increasing values of the determinant misfit $S(\mathbf{m})$. Then, the chi-square misfit $\hat{S}(\mathbf{m})$ is evaluated for the best-fitting profile [according to $S(\mathbf{m})$]. This value ($\hat{S}(\mathbf{m}_{best\,MC})$) is used as a reference value for the statistical test on the misfit $\hat{S}(\mathbf{m})$ for the evaluation of the other profiles. The procedure is applied to Monte Carlo results ordered by misfit until the test fails on 10 profiles in a row.

The obtained set of solutions is the set of profiles that can be considered equivalent in term of fitting of the experimental dispersion curve, accounting for data uncertainty.

The choice of a statistical test based on a different misfit function with respect to the Monte Carlo one, exploits the advantages of both misfits. The determinant misfit allows a multimodal stochastic inversion, which could not be performed using the distance between curves because of the computational cost. Moreover, the

**Table 2.** Modelling parameters.

| Model | Model length (m) | Receiver spacing (m) | Source depth (m) | Time window (s) | Sampling rate (s) | Number of elements | Element shape | Geometry |
|---|---|---|---|---|---|---|---|---|
| 1 | 2000 | 5 | 0 | 9 | 0.001 | 127 111 | Triangular | 2-D axial-symmetric |
| 2 | 2000 | 5 | 30 | 4 | 0.001 | 22 208 | Triangular | 2-D axial-symmetric |

determinant misfit allows to take into account the regions with low determinant where mode jumps occur. The Fisher test on the chi-square misfit allows a rational selection of equivalent solutions to be obtained. It will be shown that this selection is also useful to exclude solution corresponding to incorrect data interpretation (see Sestri Levante case history in Section 4.2).



**Figure 4.** Case 1: (a) best-fitting profiles; (b) dispersion curves for best models compared with the synthetic apparent dispersion curve; (c) absolute value of the Haskell–Thomson matrix determinant for the best-fitting model (white dots represent the synthetic experimental dispersion curve).

## 3 SYNTHETIC EXAMPLES

The multimodal Monte Carlo algorithm has been tested first using synthetic data generated with a finite-element code. The dispersion curves were extracted from the synthetic seismograms using frequency–wavenumber analysis (Maraschini *et al.* 2010).
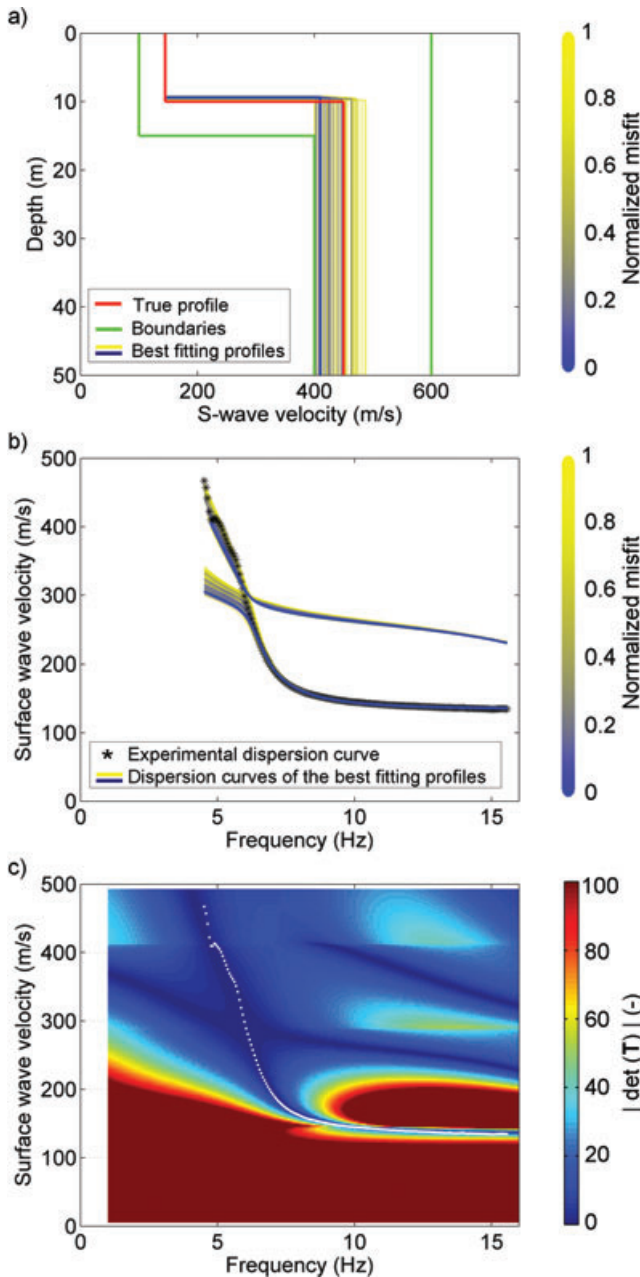
### 3.1 Case 1

The first example is a synthetic data set generated with a subsoil model composed by a soft layer over a stiffer half-space (Fig. 3). Soil parameters are summarized in Table 1, whereas the parameters of the FEM model are summarized in Table 2. The presence of a strong velocity contrast between adjacent layers typically causes a predominance of the first higher mode in the Rayleigh waves propagation. In such situations, the apparent dispersion curve shifts towards the first higher mode in the low-frequency range (Foti 2002).

The apparent dispersion curve is constituted by a single branch, with velocity included between 100 and 500 m s$^{-1}$. For the Monte Carlo inversion $2 \times 10^6$ profiles were generated between the boundaries represented in Fig. 4(a). The boundaries are selected on the basis of the velocity of propagation at low- and high-frequencies.

The algorithm finds as global minimum a model whose modal dispersion curves fit the synthetic data with the fundamental mode in the high-frequency band and with the first higher mode in the low-frequency band (Fig. 4c).

In Fig. 4(a) the best profiles are plotted using a color scale based on the fitting: blue represents the best fitting, a transition towards yellow is used to represent lower and lower misfit. The same color scale will be used consistently in the rest of the paper. The best-fitting profile is close to the theoretical profile, which is represented in red in Fig. 4(a). The other profiles selected on the basis of the statistical test represent the uncertainty associated with solution non-uniqueness. As expected, soil parameters of the first layer are better resolved than the half-space parameter. The comparison between the synthetic dispersion curve and the experimental dispersion curve, and the comparison between the synthetic dispersion curve and the absolute value of the Haskell–Thomson matrix determinant of the best-fitting model are shown in Figs 4(b) and (c), respectively.

In the real world, a soft layer overlaying a stiffer half-space is a quite common situation, for example when a shallow bedrock is present. This situation is important for seismic amplification studies. The continuity of the apparent dispersion curve also in correspondence of the mode shift makes the inversion of this kind of data challenging. An algorithm that allows all the modes to be considered without specifying to which mode each point belongs to is required for avoiding mode misidentification errors. A fundamental mode inversion would have produced sound errors in the evaluation of the $V_s$ of the half-space and on the thickness of the cover material.

### 3.2 Case 2

This data set (Fig. 5) was generated using a soil model composed by two layers over a half-space. Soil parameters are summarized in
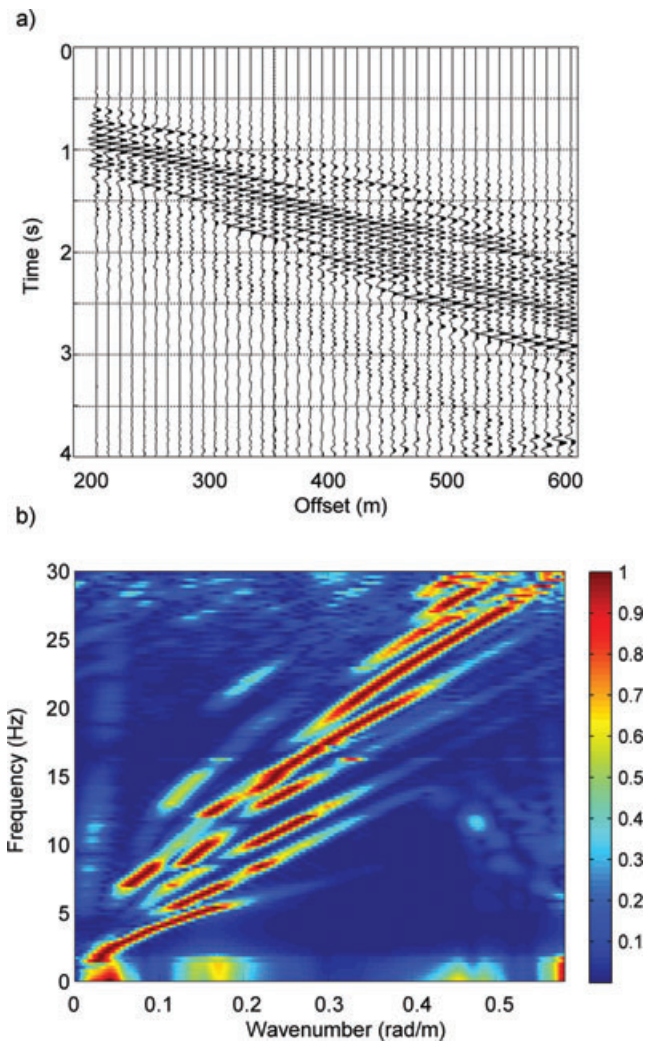
**Figure 5.** Case 2: (a) synthetic seismogram; (b) f–k spectrum.

Table 1, whereas the parameters of the FEM model are summarized in Table 2. The source is placed at the first interface. In this data set the apparent dispersion curve is composed by several branches, and, consequently, a multimodal inversion is important to exploit all available information.

Also in this case, the Monte Carlo algorithm was applied, testing $2 \times 10^6$ models. The best profiles are plotted in Fig. 6(a), while the fitting between the synthetic dispersion curve and the dispersion curves of the best profiles, and the fitting between the synthetic dispersion curve and the absolute value of the Haskell–Thomson matrix determinant of the best model, are shown, respectively, in Figs 6(b) and (c).

The best-fitting models are very close to the real model, and the distance between the real and the trial models increases when the misfit increases.

## 4  EXPERIMENTAL EXAMPLES

### 4.1  Site 1

This data set (Fig. 7) was collected at Castelnuovo Garfagnana, in central Italy. The soil deposit is composed by layers of sands, silts and well-graded gravels; the bedrock is composed by aged stiff
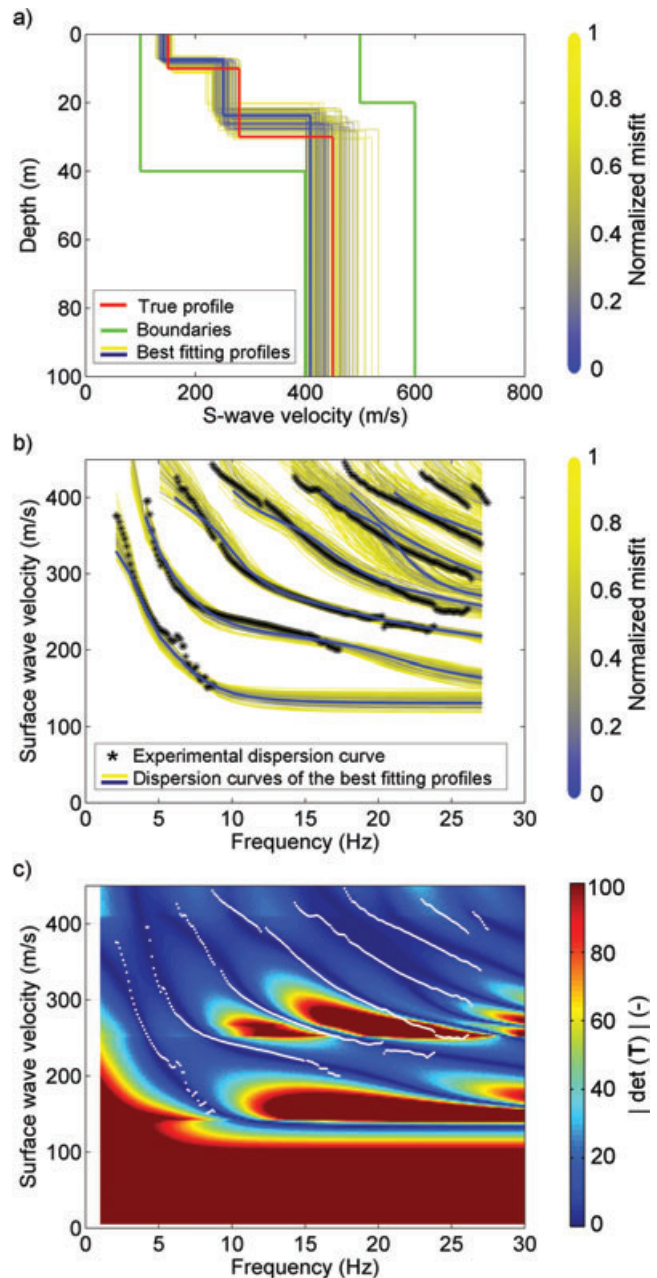


**Figure 6.** Case 2: (a) best-fitting profiles; (b) dispersion curves for best models compared with the synthetic apparent dispersion curve; (c) absolute value of the Haskell–Thomson matrix determinant for the best-fitting model (white dots represent the synthetic experimental dispersion curve).

clayey sands. A downhole test and a $S$-wave refraction surveys were performed at the same site by other surveyors.

Surface wave data were collected using a linear array; acquisition parameters are summarized in Table 3. More details on the data set and on the site are reported in Calosi *et al.* (2001).

The Monte Carlo inversion is applied generating $5 \times 10^6$ profiles within the boundaries reported in Fig. 8(a). The boundaries were selected on the basis of a preliminary and approximate inversion. In Fig. 8(a) the best profiles, according to the Fisher test, are compared to the results of the downhole and refraction tests. In Figs 8(b) and (c) the fitting between the real dispersion curve and the dispersion curves of the best profiles, and the fitting between the real
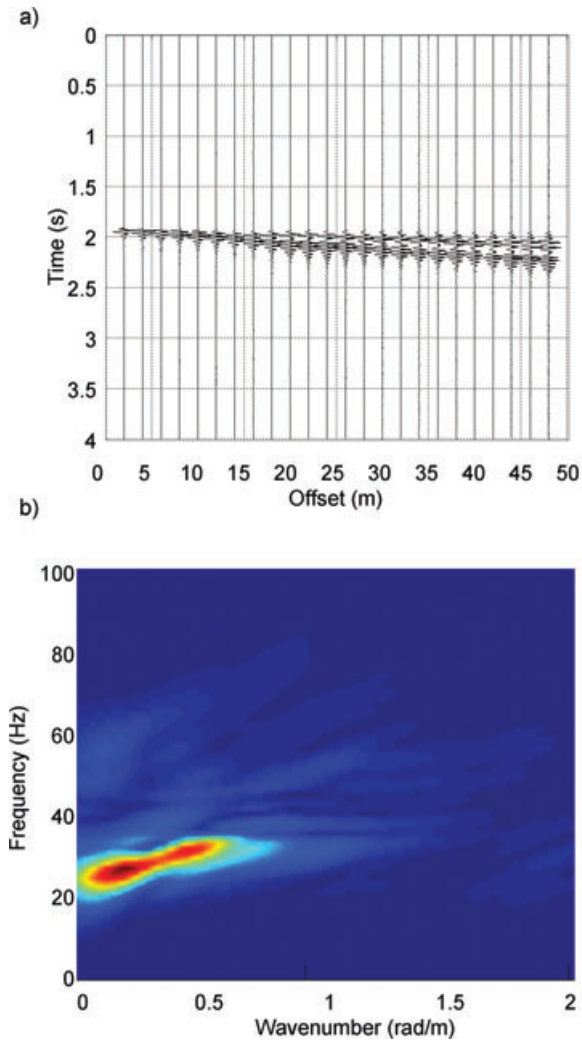
**Figure 7.** Site 1—Castelnuovo Garfagnana: (a) real data; (b) f–k spectrum.

dispersion curve and the absolute value of the Haskell–Thomson matrix determinant of the best model are, respectively, shown.

Observing Figs 8(b) and (c) a good agreement between the real data and the synthetic dispersion curve can be noted; in particular, according to the inversion, the experimental dispersion curve corresponds to the fundamental mode in the high-frequency band, and it jumps to the first higher mode in the low-frequency band.

The first interface identified by the surface wave inversion is in good agreement with downhole and refraction result; below this interface the inverted profiles show a gradual stiffness increase. The experimental dispersion curve does not show any feature that allows sound interfaces to be identified (data fitting of the inverted model is good), whereas the other methods identify a second sharp interface. This can be due to the non-uniqueness of the solution of surface wave inversion. Apparently for this situation, shear wave refraction provides more reliable information for the identification of the bedrock.
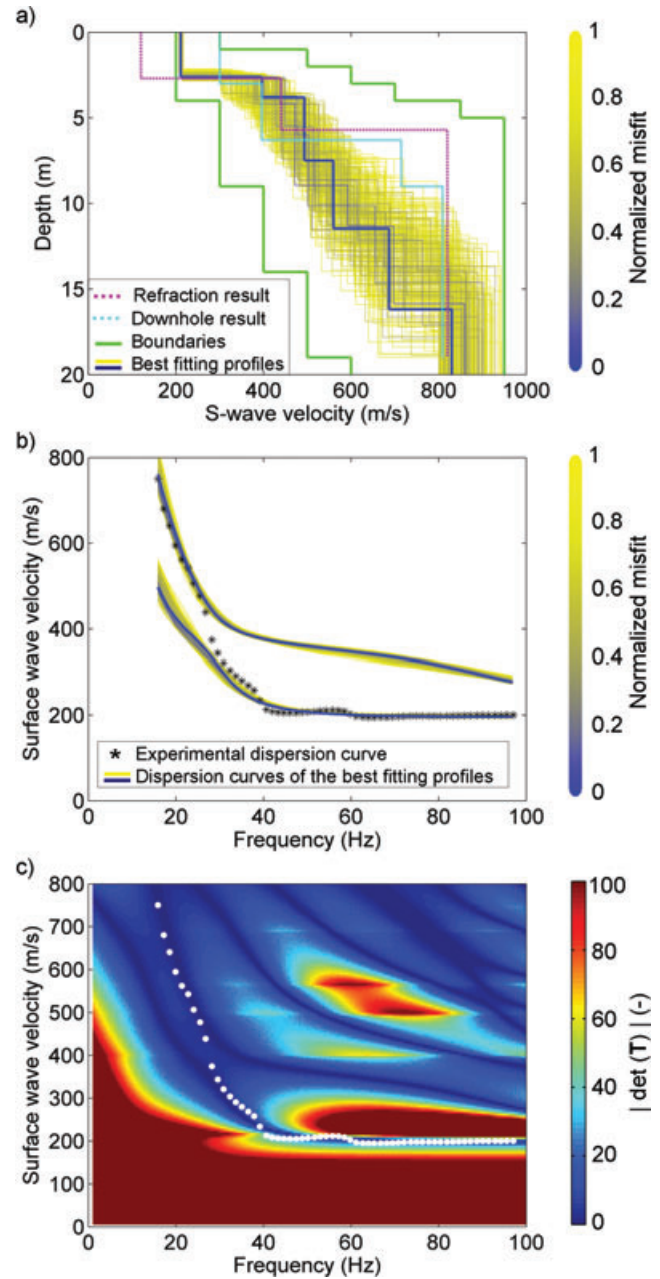


**Figure 8.** Site 1—Castelnuovo Garfagnana: (a) best-fitting profiles compared to $V_s$ profiles from a downhole test and from a refraction test; (b) dispersion curves for best models compared with the experimental dispersion curve; (c) absolute value of the Haskell–Thomson matrix determinant for best-fitting model (white dots represent the experimental dispersion curve).

### 4.2 Site 2

This data set (Fig. 9) was collected in Liguria (Italy) at the site of one of the stations of the Italian Accelerometric Network. The superficial layer is an artificially compacted layer of gravels and
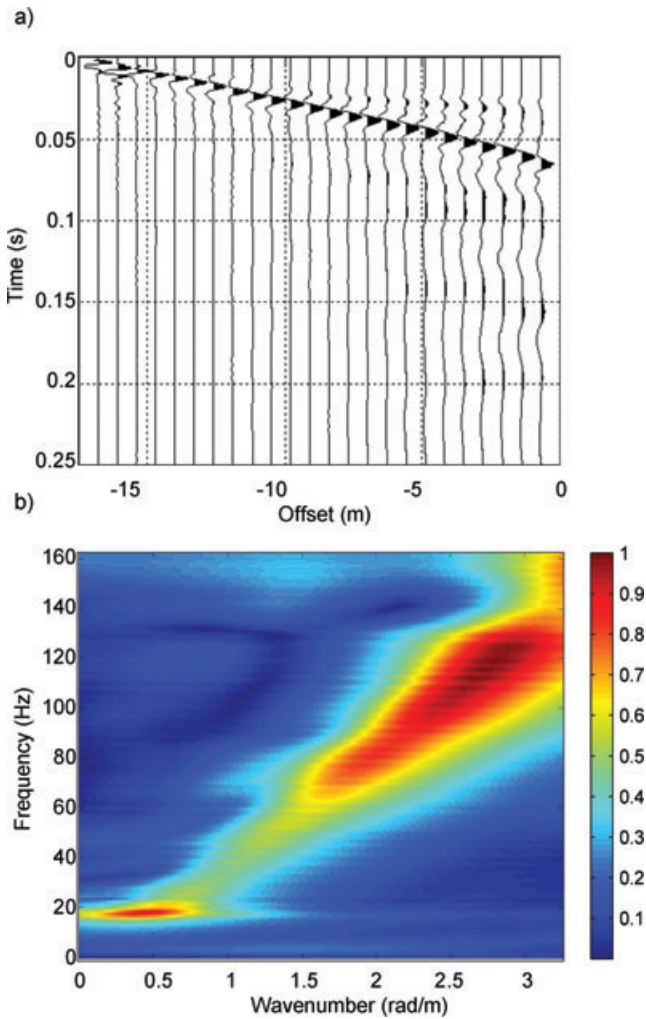
**Table 3.** Field data acquisition parameters.

| Dataset | Array length (m) | Receiver type | Receiver spacing (m) | Source type | Acquisition window (s) | Sampling rate (ms) | Number of receivers |
|---|---|---|---|---|---|---|---|
| Site 1 | 48 | Vertical 4.5 Hz | 2 | 130 kg drop weight | 4.096 | 8 | 24 |
| Site 2 | 16.4 | Vertical 4.5 Hz | 0.7 | 5 kg sledge hammer | 0.512 | 2 | 24 |

**Figure 9.** Site 2—Sestri Levante: (a) real data; (b) f–k spectrum.

pebbles used for the passage of lorries. The bedrock is expected to be close to the ground surface.

A velocity increase with frequency can be observed in the experimental dispersion curve (Fig. 10b), suggesting the presence of a velocity inversion in the subsoil model. In this condition the apparent dispersion curve follows the higher modes in the high-frequency band (Tokimatsu 1997; Foti *et al.* 2000).

Data were inverted generating $10^7$ random profiles; the best profiles selected by the Fisher test are plotted in Fig. 10(a). The solutions present a velocity inversion in the shallow portion of the soil profile. The stiff top layer is coherent with available information on the site. The fitting between the observed dispersion curve and the dispersion curve of the best profiles is very good (Figs 10b and c).

This data set is particularly challenging for a surface wave inversion algorithm because the apparent dispersion curve, composed by a single branch, follows higher modes both in the low-frequency band (because of the stiff bedrock) and in the high-frequency band (because of the stiff top layer), with a smooth transition, and consequently the mode numbering identification of the data points is impossible. Higher mode inversion increases penetration depth, because low-frequency points belong to a higher mode, and avoids sound mistakes due to mode misidentification.

In this example the use of the determinant misfit is important for the inversion of the experimental dispersion curve, and a mis-
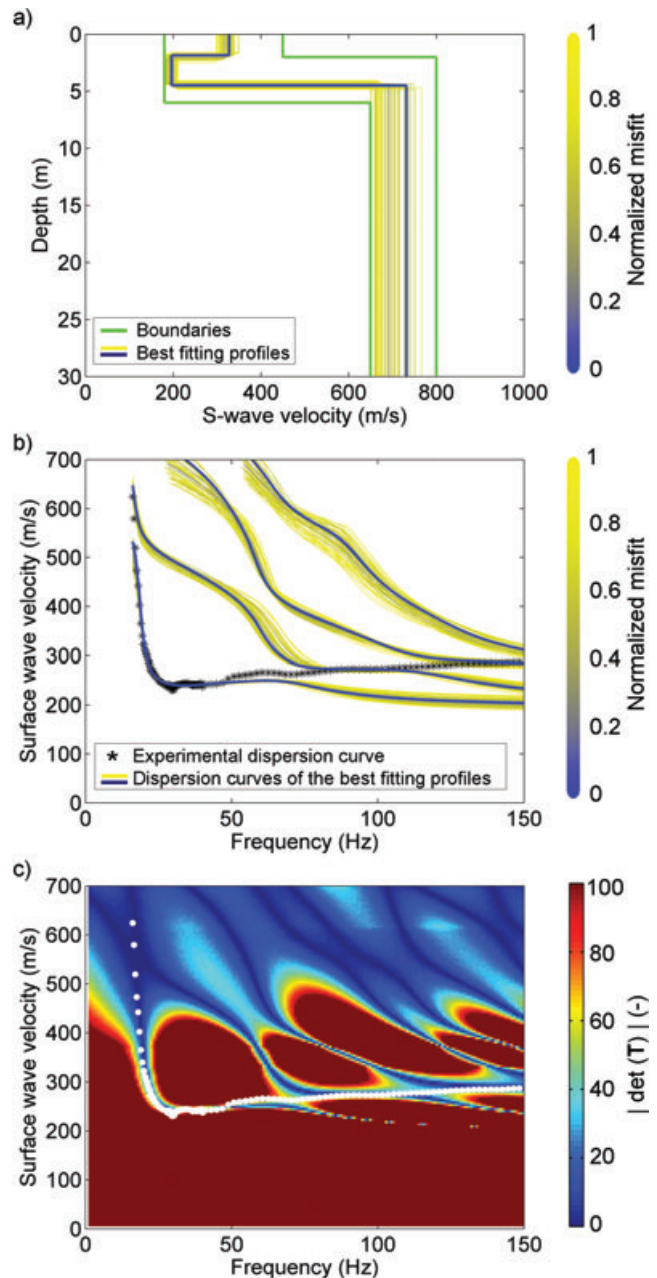


**Figure 10.** Site 2—Sestri Levante: (a) best-fitting profiles; (b) dispersion curves for best models compared with the experimental dispersion curve; (c) absolute value of the Haskell–Thomson matrix determinant for best-fitting model (white dots represent the experimental dispersion curve).

fit based on the distance between the experimental and the modal dispersion curve can create some problems in the inversion. The experimental dispersion curve is composed by the fundamental mode and the higher modes, as it can be observed in Figs 10(b) and (c), but some points of the experimental dispersion curve do not belong to any mode. They belong to transition zones because of the spatial resolution of the acquisition. A misfit function based on the distance between curves cannot handle these points correctly, because they are distant from the modes and they increase the misfit associated with a given model. On the contrary, the determinant misfit function allows to consider transition zones. The regions where the experimental dispersion curve passes from a mode to the following one are associated with low-misfit values (Fig. 10c).
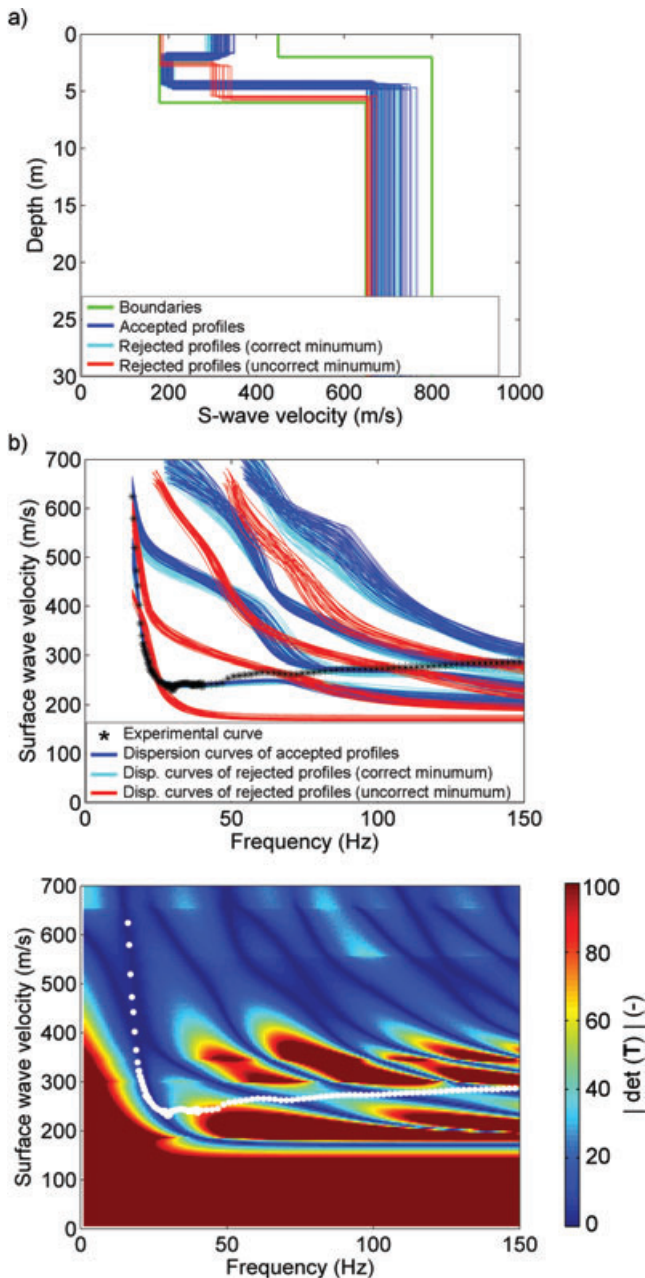
**Figure 11.** Site 2—Sestri Levante: (a) best-fitting profiles with the rejected profiles; (b) dispersion curves of soil profiles reported in (a) compared with the experimental dispersion curve; (c) absolute value of the Haskell–Thomson matrix determinant for the red profile reported in (a) associated with the low value of the determinant misfit (white dots represent the experimental dispersion curve).

On the other hand, the use of the determinant misfit function alone can lead to incorrect local minima. In Fig. 11(a) all the models whose chi-square misfit $\hat{S}(\mathbf{m})$ were evaluated are plotted. Blue models are the ones accepted by the Fisher test. Cyan models are models rejected by the test because their dispersion curve is too far from the experimental one, but they are anyway compatible with the selected models because they belong to the same class of local minima. Red models are models with a low value of the determinant misfit but they are associated to a different class of local minima. The corresponding dispersion curves are shown in Fig. 11(b). In Fig. 11(c) the absolute value of the determinant of the red profile of

Fig. 11(a) with the lowest determinant misfit is shown. The experimental dispersion curve passes in the minima of the determinant, even if it is far from all the modes of the synthetic dispersion curve; consequently the determinant misfit for this profile is low, whereas the chi-square misfit value is high.

The integrated use of the two-misfit distance allows to mitigate the problems of local minima and of mode jumps of the two-misfit functions considered independently.

## 5 CONCLUSIONS

In this work, we propose a Monte Carlo algorithm for surface wave inversion based on a multimodal misfit function.

The chosen determinant misfit function presents two main advantages. The main one is that it allows all the experimental modes to be considered in the inversion, without the need to number the modes before the inversion. The second advantage is that the computation of the misfit is faster than the usual misfit functions that require the evaluation of dispersion curves. The expensive zero search used for the computation of modal dispersion curve is avoided. The reduced computational cost of the forward problem makes it suitable for a stochastic algorithm that requires the evaluation of a large number of models.

The effectiveness of the proposed algorithm is shown by means of real and synthetic examples, where the algorithm is tested by inverting dispersion curves that present difficulties, such as passages of the apparent dispersion curve to higher modes both in the low- and high-frequency bands.

The population of profiles is used to select equivalent solutions on the basis of a statistical test, and it provides an insight into uncertainties associated with solution non-uniqueness. The integrated use of the two-misfit distances mitigates the risk of falling into local minima.

A further development could be the implementation of the same misfit function within a more efficient stochastic algorithm with a further reduction of computational costs.

## REFERENCES

Buchen, P.W. & Ben-Hador, R., 1996. Free-mode surface-wave computations, *Geophys. J. Int.,* **124**(3), 869–887.

Calosi, E., *et al.* 2001. Geological and geotechnical investigations for the seismic response analysis at Castelnuovo Garfagnana in Central Italy, *15th International Conference on Soil Mechanics & Geotechnical Engineering,* Technical Commitee 4 Special Volume, 141–148.

Curtis, A. & Lomax, A., 2001. Prior information, sampling distributions, and the curse of dimensionality, *Geophysics,* **66**(2), 372–378.

Dunkin, J., 1965. Computation of modal solutions in layered, elastic media at high frequencies, *Bull. seism. Soc. Am.,* **55**(2), 335–358.

Dziewonski, A.M. & Hales, A.L., 1972. Numerical analysis of dispersive seismic waves, in *Methods in Computational Physics,* Vol. 11, pp. 39–86, ed. Bolt, B.A., Academic Press, New York.

Ernst, F., 2007. Long-wavelength statics estimation from guided waves, in Proceedings of the 69th EAGE Conference and Exhibition, Extended Abstracts, E033, London, UK.

Ernst, F., 2008. Multi-mode inversion for Vp and thick near-surface layers, in Proceedings of the *Near Surface 2008 14th European Meeting of Environmental and Engineering Geophysics,* Kraków, Poland.

Forbriger, T., 2003a. Inversion of shallow-seismic wavefields. Part I. Wavefield transformation, *Geophys. J. Int.,* **153**(3), 719–734.

Forbriger, T., 2003b. Inversion of shallow-seismic wavefields. Part II. Inferring subsurface properties from wavefield transformation, *Geophys. J. Int.,* **153**(3), 735–752.

Foti, S., Lancellotta, R., Sambuelli, L. & Socco, L.V., 2000. 'Notes on fk analysis of surface waves', *Annali di Geofisica,* **43**(6), 1199–1210.

Foti, S., 2002. Numerical and experimental comparison between 2-station and multistation methods for spectral analysis of surface waves, *RIG (Italian Geotech. J.),* **36**(1), 11–22.

Gabriels, P., Snieder, R., & Nolet., G., 1987. In situ measurements of Vs in sediments with higher-mode Rayleigh waves, *Geophys. Prospect.,* **35**(2), 187–196.

Ganji V., Gucunski, N. & Nazarian, S., 1998. Automated inversion procedure for spectral analysis of surface waves, *J. Geotech. Geoenviron. Eng.,* **124**(8), 757–770.

Gilbert F. & Bachus, G.E., 1966. Propagator matrices in elastic wave and vibration problems. *Geophysics,* **31,** 326–332.

Gucunski, N. & Woods, R.D., 1992. Numerical simulation of the SASW test, *Soil Dyn. Earthq. Eng.,* **11**(4), 213–227.

Haskell, N., 1953. The dispersion of surface waves on multilayered media, *Bull. seism. Soc. Am.,* **43**(1), 17–34.

Haskell, N., 1964. Radiation pattern of surface waves from point sources in a multilayered medium, *Bull. seism. Soc. Am.,* **54**(1), 377–393.

Herrmann, R.B., 2002. SURF code, http://www.eas.slu.edu/People/RBHerrmann/ (accessed 2010 April 29)

Herrmann, R.B. & Wang, C.Y., 1980. A numerical study of p-, sv- and sh-wave generation in a plane layered medium, *Bull. seism. Soc. Am.,* **70**(4), 1015–1036.

Kausel, E. & Roesset, J.M., 1981. Stiffness matrices for layered soils, *Bull. seism. Soc. Am.,* **71,** 1743–1761.

Kennet, B., 1974. Reflection, rays and reverberation, *Bull. seism. Soc. Am.,* **64,** 1685–1696.

Kennet, B. & Kerry, N., 1979. Seismic wave in a stratified halfspace, *Geophys. J. R. astr. Soc.,* **57,** 557–583.

Kramer, S.L., 1996. *Geotechnical Earthquake Engineering,* xviii, Prentice Hall, Upper Saddle River, NJ, 653pp.

Lai, C.G. & Rix, G.J., 1999. Inversion of multi-mode effective dispersion curves, in *Pre-Failure Deformation Characteristics of Geomaterials,* pp. 411–418, eds Jamiolkowski, M. , Lancellotta, R. & Lo Presti, D., Balkema, Rotterdam.

Lai, C.G., Foti, S. & Rix, G.J., 2005. Propagation of data uncertainty in surface wave inversion, *J. Eng. Env. Geophys.,* **10,** 219–228.

Lu, L. & Zhang, B., 2006. Inversion of Rayleigh waves using a genetic algorithm in the presence of a low-velocity layer, *Acoust. Phys.,* **52**(60), 701–712.

Luo, Y., Xu, Y., Liu, Q. & Xia, J., 2008. Rayleigh-wave dispersive energy imaging and mode separating by high resolution linear Radon transform. *Leading Edge,* **27**(110), 1536–1542.

Maraschini, M., Ernst, F., Foti, S. & Socco, L.V., 2010. A new misfit function for multimodal inversion of surface waves, *Geophysics,* in press, doi:10.1190/1.3436539.

Mari, J.L., 1984. Estimation of static corrections for shear-wave profiling using the dispersion properties of Love waves, *Geophysics,* **49**(80), 1169–1179.

Mc Mechan, G.A. & Yedlin, M.J., 1981. Analysis of dispersive waves by wave field transformation, *Geophysics,* **46**(6), 869–874.

Menke, W., 1989. (Revised). Geophysical data analysis: discrete inverse theory, *International Geophysics Series,* Academic Press, New York.

Mosegaard, K. & Tarantola, A., 1995. Monte Carlo sampling of solutions to inverse problems, *J. geophys. Res.,* **100**(B70) 12431–12447.

Nolet, G & Panza, G.F., 1976. Array analysis of seismic surface waves: limits and possibilities, *Pure appl. Geophys.,* **114**(5), 775–790.

Park, C.B., Miller, R.D. & Xia, J., 1999, Multimodal analysis of high frequency surface wave, in *Proceedings of the Symposium on the Application of Geophysics to Engineering and Environmental Problems (SAGEEP 99),* 14–18 March 1999, pp. 115–122, Environmental and Engineering Geophysical Society, Oakland, CA.

Ryden, N. & Park, C.B., 2006. Fast simulated annealing inversion of surface waves on pavement using phase-velocity spectra, *Geophysics,* **71**(4), R49–R58.

Sambridge, M., 1999a. Geophysical inversion with a neighbourhood algorithm. Part I. Searching a parameter space, *Geophys. J. Int.,* **138,** 479–494.

Sambridge, M., 1999b. Geophysical inversion with a neighbourhood algorithm. Part II. Appraising the ensemble, *Geophys. J. Int.,* **138,** 727–746.

Sambridge, M. & Mosegaard, K. 2002. Monte Carlo methods in geophysical inverse problems, *Rev. Geophys.,* **40**(3), 1–29.

Sen, M.K. & Stoffa, P.L., 1996. Bayesian inference, Gibbs' sampler and uncertainty estimation in geophysical inversion, *Geophys. Prospect.,* **44**(20) 313–350.

Socco, L.V. & Strobbia, C., 2004. Surface wave methods for near-surface characterisation: a tutorial, *Near Surf. Geophys.,* **2**(4), 165–185.

Socco, L.V. & Boiero, D., 2008. Improved Monte Carlo inversion of surface wave data, *Geophys. Prospect.,* **56**(3), 357–371.

Song, X. & Gu, H., 2007. Utilization of multimode surface wave dispersion for characterizing roadbed structure, *J. appl. Geophys.,* **63**(2), 59–67.

Tarantola, A., 2005. Inverse Problem Theory and Methods for Model Parameter Estimation, Soc. Industrial and Applied Mathematics, Philadelphia, PA, 342pp.

Tarantola, A. & Valette, B., 1982. Inverse Problems = Quest for Information. *J. Geophys.,* **50,** 159–170.

Thomson, W.T., 1950. Transmission of elastic waves through a stratified solid medium, *J. appl. Phys.,* **21,** 89–93.

Tokimatsu, K., 1997. Geotechnical site characterization using surface waves, in *Proceedings of the First International Conference on Earthquake Geotechnical Engineering,* pp. 1333–1368, IS-Tokyo′95, Tokyo, Balkema, Rotterdam.

Tokimatsu, K., Tamura, S. & Kojima, H., 1992. Effects of multiple modes on Rayleigh wave dispersion characteristics, *J. Geotech. Eng.,* **118**(10), 1529–1543.

Xia, J., Miller, R.D., Park, C.B. & Tian, G., 2003. Inversion of high frequency surface waves with fundamental and higher modes. *J. appl. Geophys.,* **52**(1), 45–57.

Xia, J., Xu, Y., Chen, C., Kaufmann, R.D. & Luo, Y., 2006. Simple equations guide high-frequency surface-wave investigation techniques, *Soil Dyn. Earthq. Eng.,* **26**(5), 395–403.

Xu, Y., Xia, J. & Miller, R.D., 2006. Quantitative estimation of minimum offset for multichannel surface-wave survey with actively exciting source, *J. appl. Geophys.,* **59**(2), 117–125.

Zhang, S.X. & Chan, L.S., 2003. Possible effects of misidentified mode number on Rayleigh wave inversion, *J. appl. Geophys.,* **53**(1), 17–29.